Driving the SEPCaster Model with an Automated AR Identification and Characterization Module

Sailee M. Sawant[1], Gang Li[1], and Meng Jin[2]

[1]Department of Space Science and CSPAR, University of Alabama in Huntsville, Huntsville, AL 35899, USA
[2]Lockheed Martin Solar and Astrophysics Laboratory, Palo Alto, CA 94304, USA

SCIENTIFIC BACKGROUND

Solar flares and coronal mass ejections (CMEs) can cause disruptive space weather conditions, including geomagnetic storms and solar energetic particle (SEP) events, which may severely damage ground- and space-based technological systems and affect our daily lives. Therefore, we require state-of-the-art forecasting models to accurately predict space weather phenomena. **This research aims to develop a physics-based operational SEP forecast model, SEPCaster, for the energetic particle radiation environment in the inner Solar System and Earth's magnetosphere.**

SEPCaster MODEL

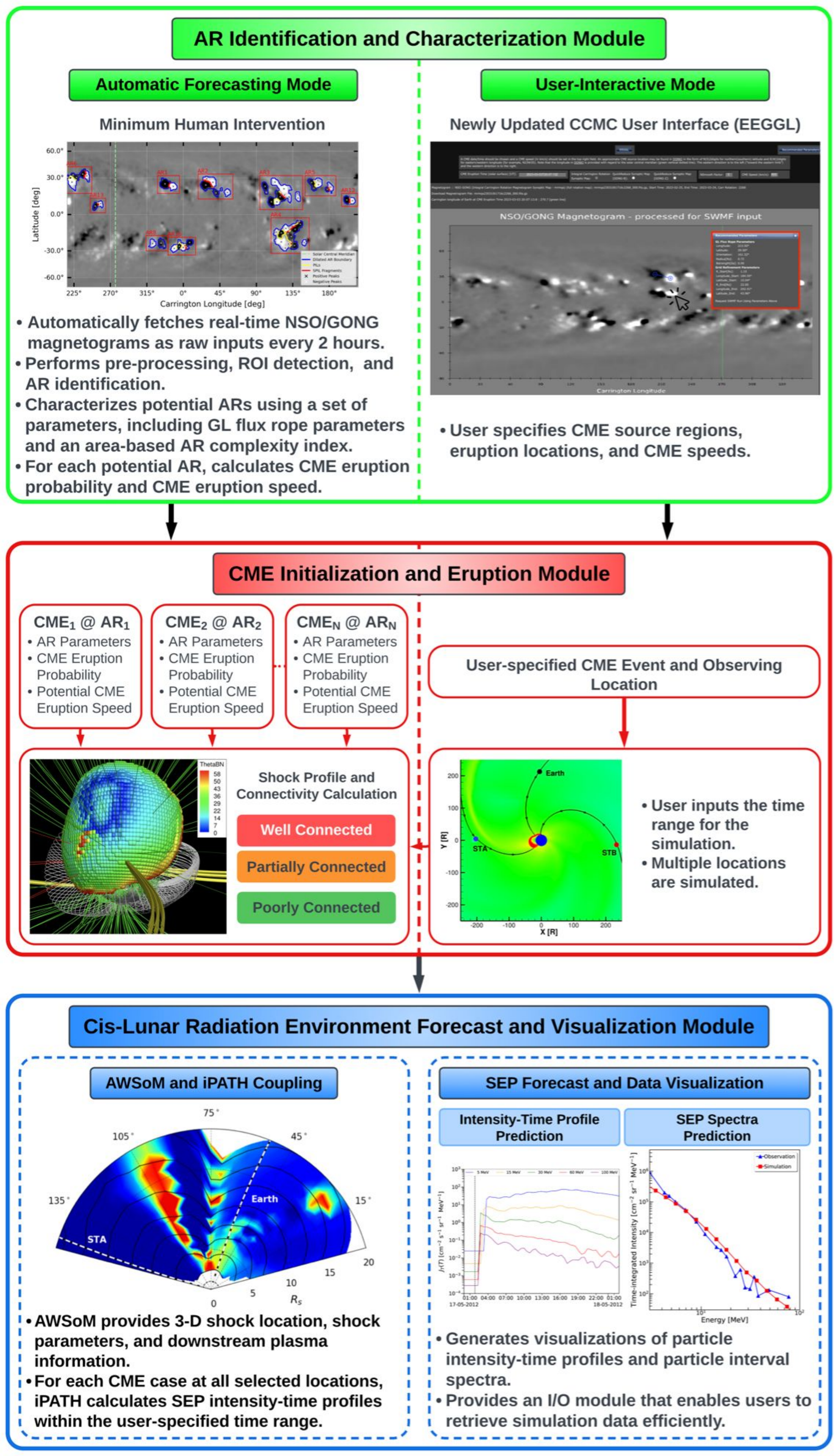

This presentation focuses on our new automated module (shown in green) for identifying and characterizing solar active regions (ARs).

ROI DETECTION

- Pre-processes the acquired NSO/GONG magnetogram by applying a **Gaussian smoothing** filter with a 5 x 5 kernel. This step suppresses the complexity of the magnetic field configuration[1].
- Uses `photutils.segmentation`[2], an affiliated package of AstroPy[3], to detect positive and negative regions of interest (ROIs) with pixel values greater than pre-defined intensity thresholds (e.g., 1σ, 2σ, and 3σ). We apply a combination of **multi-thresholding**[2] and **watershed segmentation**[2] techniques to deblend relatively complex ROIs at an intensity threshold of 1σ.
- Computes **flux-weighted centroids** of the detected ROIs.
- Implements **structural thresholding** and removes ROIs smaller than a pre-defined area threshold (e.g., 10 pix^2).

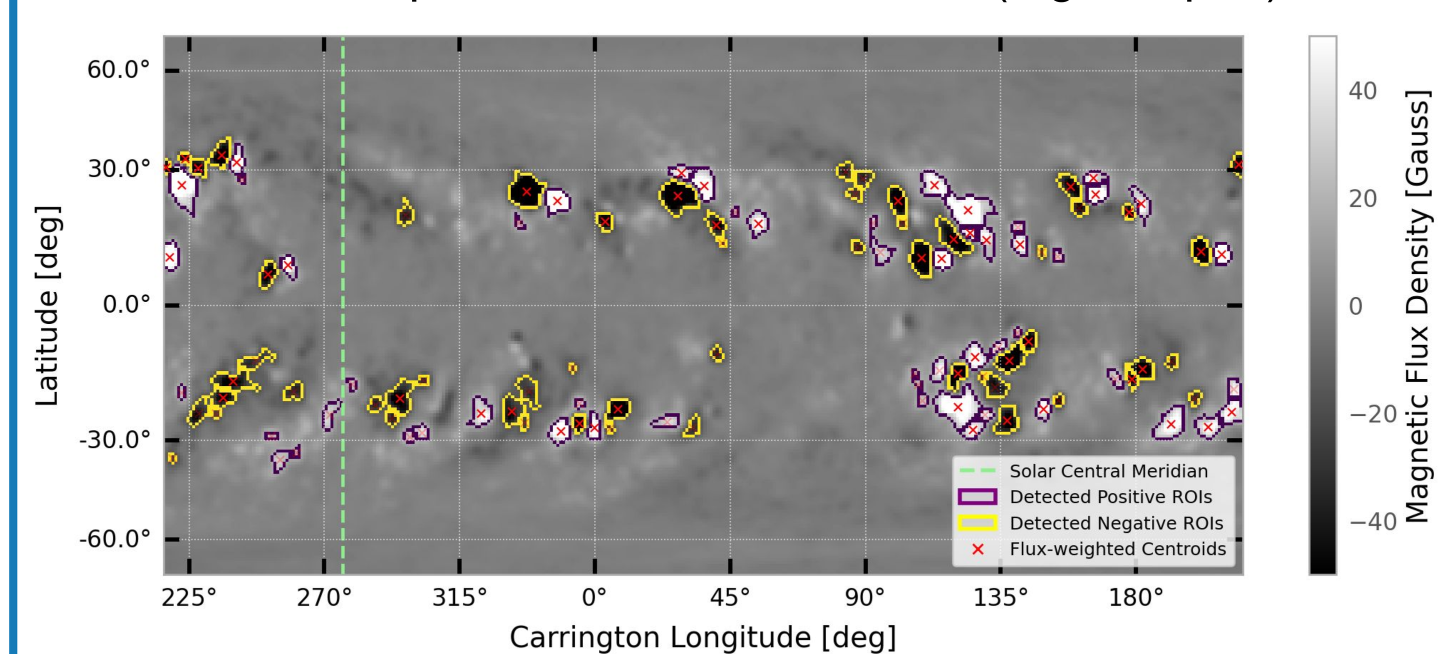

Figure 1: Pre-processed NSO/GONG MRBQS magnetogram for Carrington Rotation 2268 obtained on March 03, 2023 at 11:04 UT. Positive and negative ROIs are detected at an intensity threshold of 1σ.

AR IDENTIFICATION

- Implements an **agglomerative hierarchical algorithm**[4] to identify potential ARs from the detected ROIs.
  - Determines the optimal number of clusters by calculating the silhouette score[5], root-square[6], and root-mean-square-standard deviation[6] indices for each hierarchical level.
- Refines the results by:
  - Calculating the **separation probability** of ROIs within the acquired clusters.
  - Adding ungrouped ROIs to the acquired clusters using the **area-distance correlation criterion.**
  - Imposing the **flux-cancellation mechanism criterion**.
  - Verifying that each cluster contains at least one ROI of **opposite polarity**.

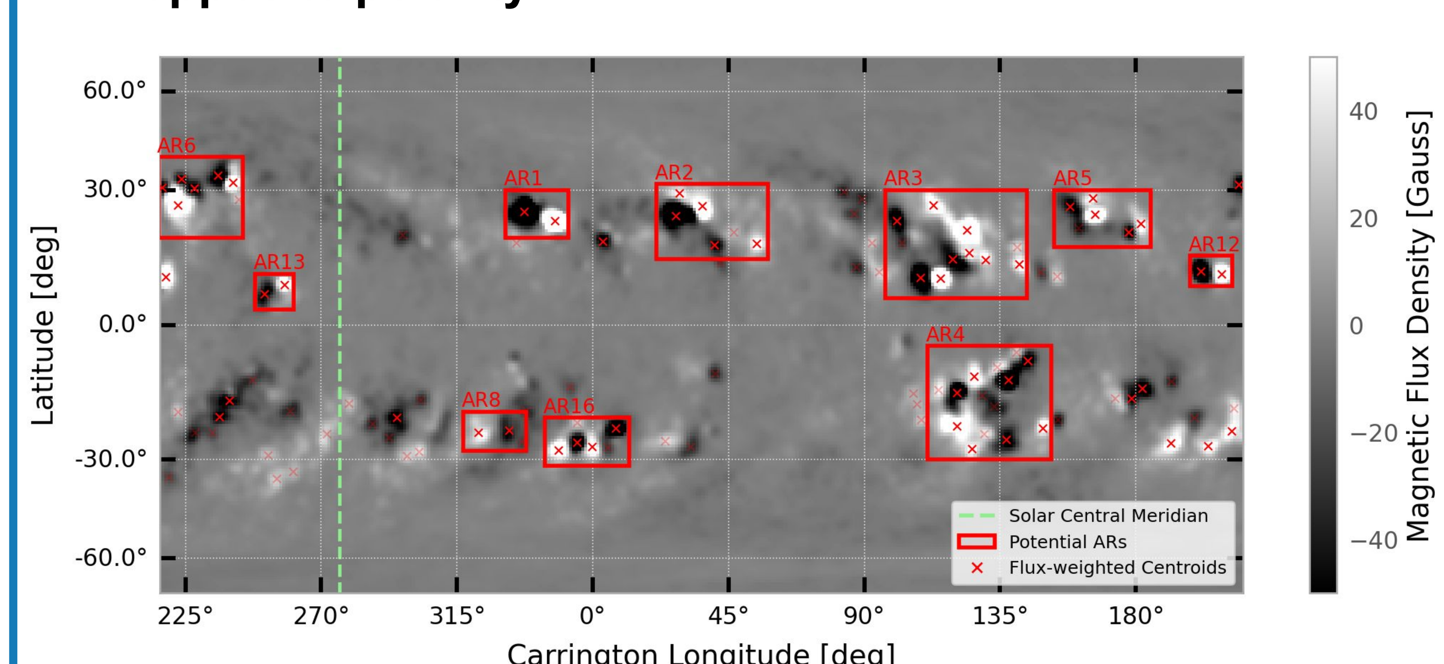

Figure 2: Potential ARs (red boxes) for the pre-processed NSO/GONG MRBQS magnetogram shown in Figure 1.

AR CHARACTERIZATION

- Characterizes the identified potential ARs using **parameters listed in Table 1 of Steward et. al. (2017)**. Some of the important parameters include number of flux peaks, maximum unsigned flux, total area, number of polarity inversion lines (PILs) and strong-gradient PILs, length of PILs and SPILs, and longitudinal and latitudinal gradients.
- Calculates AR complexity indices using our modified version of **correlation dimension mapping**[7] **(CDM)**.

BOUNDARY- AND AREA-BASED AR COMPLEXITY INDICES

Mason & Uritsky (2022) originally introduced CDM to quantify the irregularities in coronal hole boundaries. We extend the application of CDM to ARs and define our own boundary- and area-based AR complexity indices. This provides a way to characterize the identified ARs and helps in determining their potential for eruptive activity.

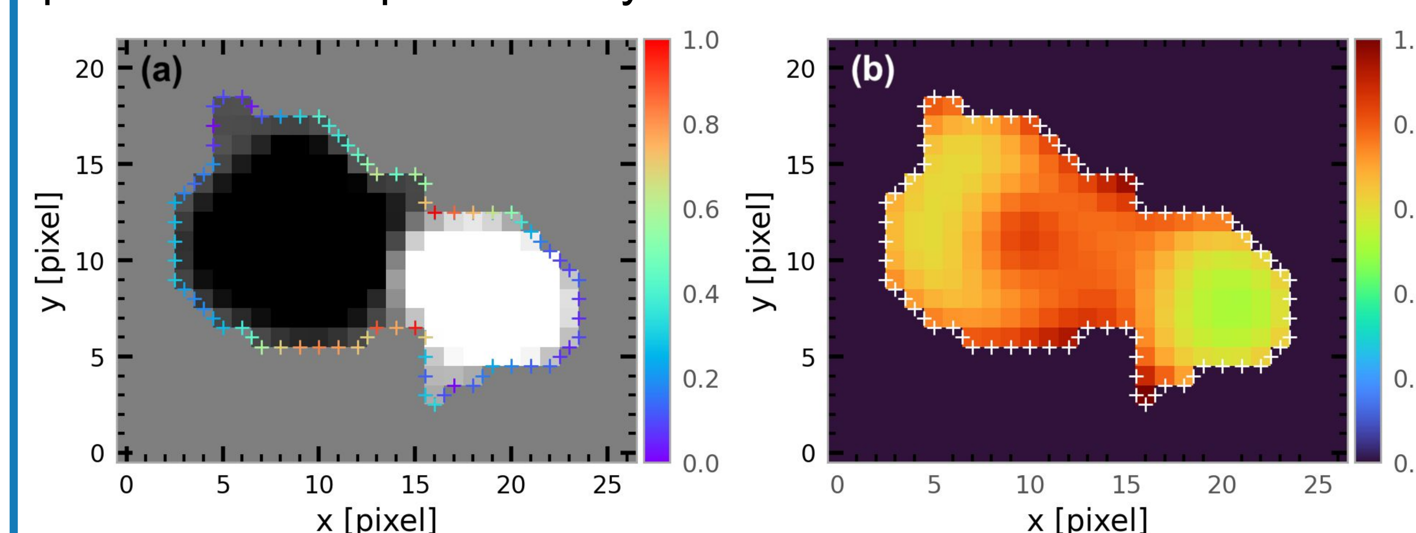

Figure 3: Examples of normalized (a) boundary- and (b) area-based CDMs for AR1 identified in Figure 2. The average boundary- and area-based CDM indices for AR1 are 1.575 and 1.593, respectively.

POTENTIAL CME ERUPTION SPEED

Based on an empirical model presented in Georgoulis (2008), we calculate the potential CME eruption speed as follows:

$$\Phi_{tot}\,[\mathrm{Mx}] = \iint B^2/B_{avg}\,dS \qquad B_{eff}\,[\mathrm{G}] \approx c\,10^{-21.96}\Phi_{tot}^{1.08} \qquad V_{CME}\,[\mathrm{km/s}] \approx 87.3 B_{eff}^{0.38}$$

where c is the fraction of the length of SPILs to total PILs. For AR1 in Figure 2, we obtained V_{CME} ≃ 674 km/s, while CACTus[8] reported the median and maximum speeds of 637 km/s and 1948 km/s, respectively. A better empirical formula will be examined in future work.

REFERENCES

[1] Jin, M., Manchester, W. B., van der Holst, B., et al. 2017, The Astrophysical Journal, 834, 173, doi: 10.3847/1538-4357/834/2/173
[2] Bradley, L., Sipőcz, B., Robitaille, T., et al. 2022, astropy/photutils: 1.5.0, 1.5.0, Zenodo, doi: 10.5281/zenodo.6825092
[3] Astropy Collaboration, Price-Whelan, A. M., Lim, P. L., et al. 2022, ApJ, 935, 167, doi: 10.3847/1538-4357/ac7c74
[4] Pedregosa, F., Varoquaux, G., Gramfort, A., et al. 2011, Journal of Machine Learning Research, 12,2825
[5] Rousseeuw, P. J. 1987, Computational and Applied Mathematics, 20, 53, doi: 10.1016/0377-0427(87)90125-7
[6] Sharma, S. 1996, Applied Multivariate Techniques (New York: Wiley), 225, doi: 10.1002/9780470316757
[7] Mason, E. I., & Uritsky, V. M. 2022, The Astrophysical Journal Letters, 937, L19, doi: 10.3847/2041-8213/ac9124
[8] Robbrecht, E., Berghmans, D., & Van der Linden, R. A. M. 2009, ApJ, 691, 1222, doi: 10.1088/0004-637X/691/2/1222
[9] Steward, G., Lobzin, V., Cairns, I. H., Li, B., & Neudegg, D. 2017, Space Weather, 15, 1151, doi: 10.1002/2017SW001595
[10] Georgoulis, M. K. 2008, Geophysical Research Letters, 35, L12102, doi: 10.1029/2007GL032040

ACKNOWLEDGEMENTS

This research is supported in part by NASA 80NSSC22K0268 and NSF ANSWERS 149771.

THE UNIVERSITY OF ALABAMA IN HUNTSVILLE